



## Calorimetric and optical investigation of the nematic, splay-nematic, and ferroelectric nematic phases of RM734 liquid crystal

Marta Lavrič, Nerea Sebastián, Calum J Gibb, Richard J Mandle, Alenka Mertelj, Nikola Novak & George Cordoyiannis

To cite this article: Marta Lavrič, Nerea Sebastián, Calum J Gibb, Richard J Mandle, Alenka Mertelj, Nikola Novak & George Cordoyiannis (19 Mar 2025): Calorimetric and optical investigation of the nematic, splay-nematic, and ferroelectric nematic phases of RM734 liquid crystal, Liquid Crystals, DOI: [10.1080/02678292.2025.2481076](https://doi.org/10.1080/02678292.2025.2481076)

To link to this article: <https://doi.org/10.1080/02678292.2025.2481076>



© 2025 The Author(s). Published by Informa UK Limited, trading as Taylor & Francis Group.



Published online: 19 Mar 2025.



Submit your article to this journal [↗](#)



Article views: 399










View related articles [↗](#)



View Crossmark data [↗](#)

# Calorimetric and optical investigation of the nematic, splay-nematic, and ferroelectric nematic phases of RM734 liquid crystal

Marta Lavrič <sup>a</sup>, Nerea Sebastián <sup>b</sup>, Calum J Gibb <sup>c</sup>, Richard J Mandle <sup>c,d</sup>, Alenka Mertelj <sup>b</sup>, Nikola Novak <sup>a</sup> and George Cordoyiannis <sup>a</sup>

<sup>a</sup>Condensed Matter Physics Department, Jožef Stefan Institute, Ljubljana, Slovenia; <sup>b</sup>Department of Complex Matter, Jožef Stefan Institute, Ljubljana, Slovenia; <sup>c</sup>School of Chemistry, University of Leeds, Leeds, UK; <sup>d</sup>School of Physics and Astronomy, University of Leeds, Leeds, UK

## ABSTRACT

RM734 is one of the first two liquid crystal compounds reported to exhibit the ferroelectric nematic phase. At the early stage of its characterisation, a direct nematic – to – ferroelectric nematic phase transition was reported for this compound. However, subsequent studies revealed the presence of an intermediate phase between the nematic and ferroelectric nematic ones. Here, we provide additional evidence on the calorimetric signature and the optical texture of this intermediate phase, referred to as the splay-nematic phase. Next, we briefly comment on the nature of the transitions between the nematic, splay-nematic, and ferroelectric nematic phases, and the substantially different transition temperatures reported in the literature for RM734.

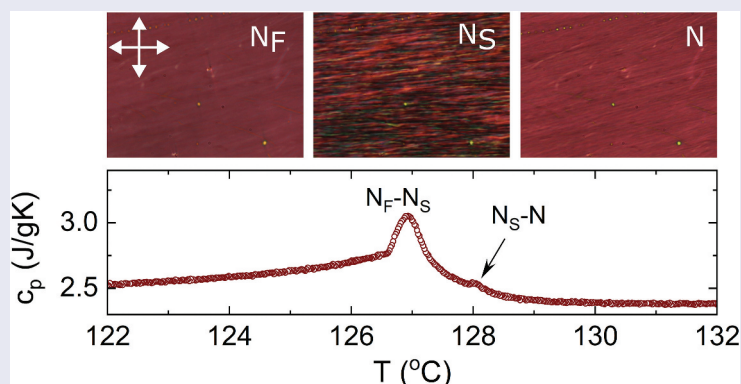
## ARTICLE HISTORY

Received 19 February 2025

Accepted 6 March 2025

## KEYWORDS

RM734 liquid crystal; ferroelectric nematic phase; splay-nematic phase; AC calorimetry; polarising optical microscopy



## Introduction

The nematic (N) phase of rod-like, thermotropic liquid crystals (LCs) appears upon cooling from the isotropic (I) phase and is characterised by high fluidity and long-range orientational order. The average N molecular alignment is along a preferred direction noted by a vector  $\hat{n}$ , the so-called director. However, the dipole moments point randomly into parallel and antiparallel directions ( $\hat{n}$ ,  $-\hat{n}$ ) leading to a zero macroscopic polarization for the N phase. A polar nematic phase was anticipated based on the theory of ferroelectric fluids developed at the beginning of the 20<sup>th</sup> century [1,2]. In 2017, Mandle et al. [3] and Nishikawa et al. [4] simultaneously reported the synthesis of the first two LCs exhibiting the ferroelectric nematic phase ( $N_F$ ), referred to as RM734 and DIO respectively.

The initial characterisation of RM734 indicated the presence of two nematic phases (N and  $N_F$ ) [3], with the transition between them being weakly first-order [5]. On the contrary, an intermediate phase was identified between the N and the  $N_F$  phases of DIO [4], with a temperature range of ~16.8 K derived by high-resolution calorimetry [6]. The possibility of the existence of this intermediate phase in the case of RM734 has been conjectured by Sebastian et al. [7], based on the observation of subtle changes in the flickering of optical textures at the onset of the  $N_F$  phase. More recently, the thermal signature of the intermediate phase has been reported by Thoen et al. [8] for RM734 samples of different origins. The nomenclature used for this intermediate phase differs; in various studies, it is referred to as  $M_2$ ,  $SmZ_A$ ,  $N_S$ , or  $N_x$  [4,6,7,9]. Also, its exact nature remains controversial: it is addressed as either

a modulated, splay-nematic ( $N_S$ ) [7,10,11] or an anti-ferroelectric smectic phase ( $SmZ_A$ ) [9,12] with the molecules lying perpendicular to the smectic layer normal. Recently, it has been shown that doping RM734 with ions significantly expands the temperature range over which the intermediate phase is observed, revealing a splayed structure modulated in two dimensions [13]. Henceforth, we use  $N_S$  when referring to this phase.

Following the discovery of RM734 and DIO, several ferroelectric nematic LC compounds (FNLCS) have been synthesised bearing different phase sequences and exhibiting the  $N_F$  phase [14–23], or even multiple ferroelectric nematic phases [24]. Colossal dielectric permittivity and large polarisation values have been reported along the  $N_F$  phase of several of these compounds [4,25]. The discovery of FNLCS has attracted major interest for fundamental reasons and promising applications. The former relates to the measurements of intrinsic properties, the definition of the nature and the critical behaviour of new phase transitions, and the development of theoretical models with coupled order parameters [5,6,26–30]; the latter pertains to envisioned applications in ultra-fast, energy-efficient displays and photonics, as well as enhanced caloric effects [31–40].

In this brief report, we present a combined AC calorimetry and polarising optical microscopy study along the  $N-N_S-N_F$  sequence of RM734, focusing on the vicinity and along the  $N_S$  phase. The acronym AC refers to the oscillating input power of this calorimetric method. Utilizing slow calorimetric heating and cooling runs, we have revisited the phase transition behaviour of a sample previously conjectured – yet not clearly proven – to have a small range of  $N_S$  phase [7], as well as a sample from a newer batch. The  $N_S$  range obtained by the two methods, on bulk (calorimetry) and thin (microscopy) samples, is reproducible upon heating and cooling. On the contrary, the derived transition temperatures differ substantially depending on the samples' origin and batch, even when comparing precise measurements performed with slow rates. Next, we present a summary of the results in this work and recent literature findings [5,6,8] regarding the nature of the  $N_F-N_S$  and  $N_S-N$  phase transitions, as well as the inverted Landau behaviour of the former. Finally, we comment on the importance of the synthesis processes, the role of impurities on the transition temperatures, and the relative stability of these different types of nematic phases.

## Materials and methods

Two batches of RM734 samples were synthesised at the University of Leeds, UK, stored carefully and used for our measurements without any further treatment. Both samples were chemically synthesised in the same

manner. Henceforth, we refer to these samples as batch-1 and batch-2.

Polarizing optical microscopy (POM) experiments were performed in an Optiphot-2 POL Nikon microscope equipped with a Canon EOS M200 camera. Note that optical textures of batch-1 sample have been shown in a previous study by some of the authors [7], thus, we have focused on textures of batch-2. The sample was held in a heating stage, connected to MK1-Instec temperature controller that stabilised the temperature within  $\pm 10$  mK. In order to obtain the textures, the sample was filled in an EHC 5  $\mu\text{m}$ -thick liquid crystal cell with parallel rubbing at 150°C and then cooled down at a rate of 0.1 K/min under the microscope, recording the POM images through the  $N-N_S-N_F$  phase sequence.

The RM734 temperature profiles of specific heat capacity,  $c_p(T)$ , for samples from both batches were obtained using high-resolution AC calorimetry. In its common AC mode of operation, this method senses the continuous changes of enthalpy and yields the precise  $c_p(T)$  profiles in the case of second-order transitions. In the case of first-order transitions, the coexistence region is detected by an anomalous behaviour of the phase shift between the applied AC power and the temperature oscillations of the sample. To detect latent heat, an additional mode of operation, the so-called relaxation or non-adiabatic scanning mode, is often used [41,42]. The AC calorimetric apparatus at Jožef Stefan Institute (Slovenia) is home-made and automatised. It achieves thermal stability of  $\sim 50$   $\mu\text{K}$  and operates at slow scanning rates, which are important when studying phase transitions with small enthalpy content, as shown in the cases of LC blue phases and twist-grain boundary phases [43,44].

For the calorimetric measurements, sample masses of  $\sim 30$  mg (batch-1) and  $\sim 40$  mg (batch-2) were loaded in home-made cells made of high-purity silver. A small heater and a glass-bead thermistor were attached at opposite sides of the cell to supply power to the sample and accurately measure its temperature. To obtain the net  $c_p$  of RM734, the heat capacity of the empty cell was subtracted and the result was divided by the sample's mass.

## Results and discussion

Prior to the AC calorimetric measurements, both samples were heated to  $\sim 160^\circ\text{C}$  for a short time and then cooled to the starting temperature of the run at  $\sim 138^\circ\text{C}$ . The cooling and heating rates were set to 0.15 K/h near the transitions and 0.4 K/h away from them (i.e. at much

higher or much lower temperatures). A heating and a cooling run were performed for batch-1, and a cooling run for batch-2. In all measurements, two anomalies were observed, attributed to the  $N_F$ - $N_S$  and  $N_S$ -N phase transitions. More specifically, the larger sharp anomaly corresponds to the  $N_F$ - $N_S$ , and the small peak superimposed on the high-temperature  $c_p$  wing denotes the  $N_S$ -N phase transition. The  $c_p(T)$  profiles of all runs are presented in Figure 1.

A small hysteresis, in the order of  $\sim 0.6$  K, was observed for the transition temperatures of the  $N_F$ - $N_S$  and  $N_S$ -N anomalies between the slow heating and the cooling run of batch-1. Such a finite hysteresis, along with slightly anomalous phase behaviour (visible in the case of  $N_F$ - $N_S$ ), implies that these transitions are weakly first-order. This conclusion is in full agreement with the high-resolution calorimetric results obtained by Thoen et al. [5,8], who reported a weakly first-order character for both the  $N_F$ - $N_S$  and the  $N_S$ -N transitions, with small – but still clearly measurable – involved latent heat. For clarity, it should be noted that in these studies the intermediate phase was designated as  $N_x$  (instead of

$N_S$  in the present study). The temperature range of the  $N_S$  phase for the batch-1 sample, calculated as the average of the heating and cooling run, is  $\Delta T_{NS} = 1.07 \pm 0.07$  K.

Regarding the batch-2 sample, a cooling run has been performed with the same scanning rate of 0.15 K/h, for a direct comparison with batch-1. Both  $N_F$ - $N_S$  and  $N_S$ -N transitions are again observed, albeit at slightly lower ( $\sim 0.6$  K) temperatures compared to batch-1. The temperature range of the intermediate  $N_S$  phase for the batch-2 sample is  $\Delta T_{NS} = 1.07 \pm 0.10$  K, in excellent agreement with the one obtained for batch-1. Due to the smallness of the  $N_S$ -N anomaly and its superposition on the pretransitional fluctuations  $c_p(T)$  wing of the  $N_F$ - $N_S$  peak, the error in the determination of  $T_{NS-N}$  (i.e. the  $N_S$ -N transition temperature) is larger than the error of  $T_{NF-NS}$  (i.e. the  $N_F$ - $N_S$  transition temperature). The values of both transition temperatures and the range of intermediate phase per batch are summarised in Table 1.

As mentioned before, the presence of a narrow intermediate phase in the case of RM734 was first speculated based on subtle changes in the optical textures when observed in thin films under slow cooling runs [7]. POM experiments reported there were performed with batch-1, and showed a narrow temperature interval between the N and the  $N_F$  phase in which freezing of the flickering could be observed (see Figure 7 and Supplementary Movie 2 in reference [7]). It should be noted that, due to the heating stage designs for microscopy, temperature gradients across the LC cell are present even under slow cooling, enabling observations of phase fronts. We performed the same experiments here with batch-2 observing two different regions, in which the temperature gradient occurs parallel (Figure 2, as in reference [7] for batch-1) or perpendicularly to the cell rubbing direction (Figure 3). On cooling (Figure 2(a)), as reported for batch-1, a stripy texture develops on approaching the phase transition, with enhanced director fluctuations, which freeze at the N- $N_S$  transition. A threaded texture then develops for a narrow temperature interval. Then the  $N_S$ - $N_F$  transition takes place, characterised by a striped front at the phase boundary, after which the texture homogenises again. The textural changes, although might appear subtle, are quite evident under slow cooling conditions and careful observation. Interestingly, on heating, the presence of an intermediate narrow  $N_S$  phase becomes even more evident (Figure 2(b)).

This is also the case when the temperature gradient occurs perpendicularly to the rubbing direction (Figure 3). Here, a clear N- $N_S$ - $N_F$  phase sequence can be observed. In this case, the N- $N_S$  phase transition is marked by the appearance of areas with different transmitted intensities between crossed polarisers suggesting

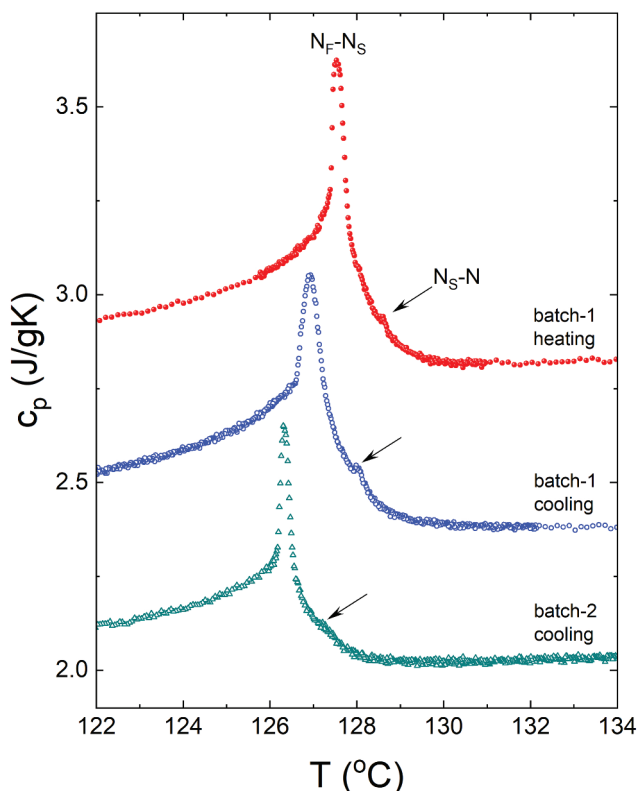


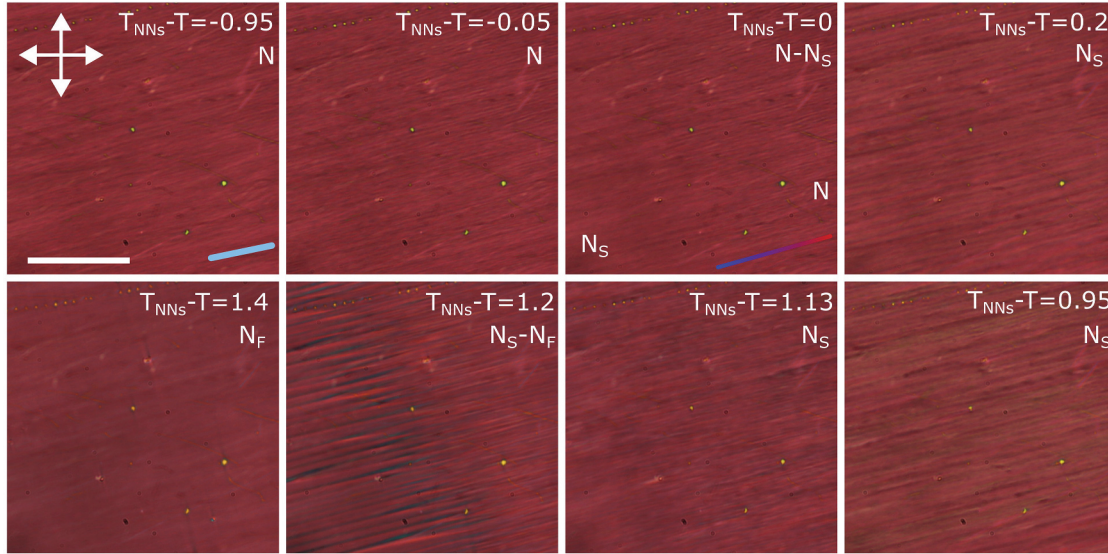
**Figure 1.** (Colour online) The temperature profiles of specific heat capacity  $c_p(T)$ , obtained with the AC calorimetry, for samples of batch-1 and batch-2. The scanning rate on heating and cooling was 0.15 K/h close to the transitions. Red solid circles: batch-1, heating run; blue open circles: batch-1, cooling run; cyan open triangles: batch-2, cooling run. The arrows denote the small anomaly associated with the  $N_S$ -N phase transition.



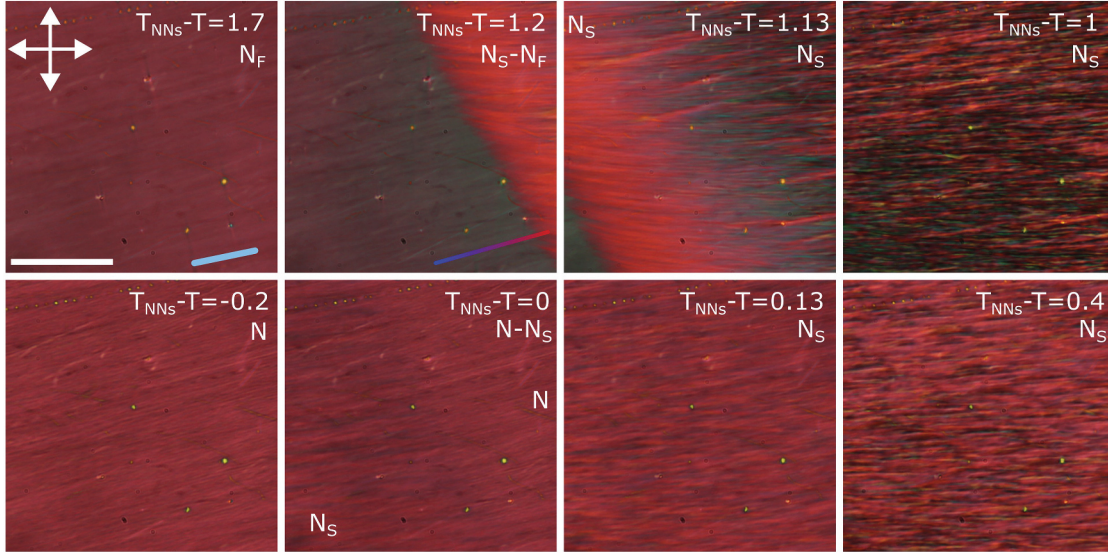
**Table 1.** A summary of the AC calorimetry runs is presented here. The sample batch, the run type and the scanning rate (near the transitions), the  $N_F$ - $N_S$  and  $N_S$ - $N$  transition temperatures,  $T_{N_F-N_S}$  and  $T_{N_S-N}$ , and the range  $\Delta T_{N_S}$  of the splay-nematic phase are shown from left to right. All transition temperatures are presented in degrees Celsius for an easier comparison with other studies.

Sample	Run type	Rate (K/h)	$T_{N_F-N_S}$ (°C)	$T_{N_S-N}$ (°C)	$\Delta T_{N_S}$ (K)
batch-1	heating	0.15	$127.53 \pm 0.02$	$128.60 \pm 0.05$	$1.07 \pm 0.05$
batch-1	cooling	0.15	$126.93 \pm 0.02$	$127.99 \pm 0.05$	$1.06 \pm 0.05$
batch-2	cooling	0.15	$126.30 \pm 0.02$	$127.37 \pm 0.10$	$1.07 \pm 0.10$

a) R ||  $\nabla T$  Cooling



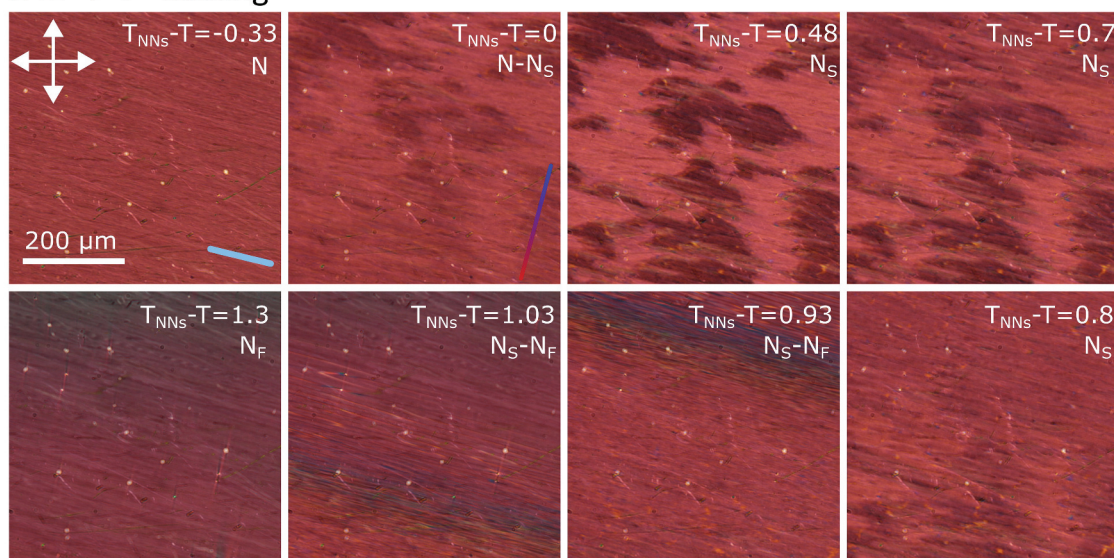
b) R ||  $\nabla T$  Heating



**Figure 2.** (Colour online) Optical textures of the  $N$ - $N_S$ - $N_F$  phase sequence observed in polarising optical microscopy for RM734, batch 2 in a 5  $\mu\text{m}$  thick EHC cell with parallel rubbing. (a) On cooling at 0.1 K/min. (b) On heating at 0.25 K/min. On both, the cooling and heating runs, the temperature gradient is along the rubbing direction. The double-headed arrows denote the crossed polarisers. The light-blue line indicates the rubbing direction and the gradient-coloured line shows the direction of the temperature gradient.

a slightly different alignment. These areas slowly homogenise on cooling at the onset of the  $N_S$ - $N_F$  phase transition. The latter is characterised by the propagation of a front with a stripy texture, which soon homogenises

into the  $N_F$  phase. From POM textures we can observe a temperature range for the  $N_S$  phase of  $\Delta T_{N_S} = 1.2 \pm 0.3$  K, which is in reasonable agreement with the AC calorimetry data.

$R \perp \nabla T$  Cooling


**Figure 3.** (Colour online) Optical textures of the N-N<sub>S</sub>-N<sub>F</sub> phase sequence observed in POM for RM734 batch 2 in a 5 μm thick EHC cell with parallel rubbing, on cooling at a rate of 0.1 K/min. The temperature gradient occurs perpendicularly to the cell rubbing direction. The double-headed arrows denote the crossed polarisers. The light-blue line indicates the rubbing direction and the gradient-coloured line shows the direction of the temperature gradient.

In Figure 4, the N<sub>F</sub>-N<sub>S</sub> and N<sub>S</sub>-N phase transition temperatures are shown for the present work and all previous studies from the literature. In some cases, the N<sub>S</sub> phase was either not detected [3,5,12] or only conjectured [7]. The adiabatic scanning calorimetry points [8] correspond to average values from all heating and

cooling runs per RM734 samples of the same origin. For the current results, separate points are used for the heating and cooling runs per sample batch. It turns out that the reported transition temperatures differ by as much as 6 K in general, and up to 4 K when comparing results from high-resolution calorimetry. For the

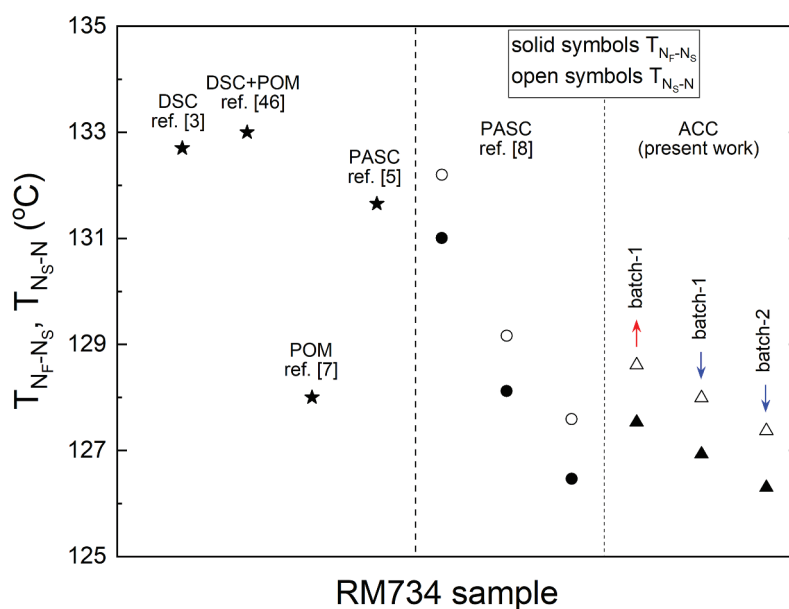


**Figure 4.** (Colour online) A comparison between the N<sub>F</sub>-N<sub>S</sub> (solid symbols) and N<sub>S</sub>-N (open symbols) transition temperatures of RM734, sourced from previous literature and the current study, is presented here. Stars [3,5,7,46] and circles [8] denote average transition temperatures taken from the literature; triangles refer to the results of this work. The experimental method employed in each case is also noted: DSC (differential scanning calorimetry); POM (polarising optical microscopy); ACC (AC calorimetry); PASC (Peltier element-based adiabatic scanning calorimetry).

latter, such large differences cannot be attributed to the thermometry (e.g. calibrations of different setups), the scanning rate, or the type of run (heating, cooling). Therefore, they must be solely related to the samples; e.g. slight difference in the amount of ionic impurities present or the timescale each sample was held at high temperatures during the experiments. Recent studies have indeed revealed that even mild doping of RM734, as well as DIO, with ionic impurities, can change their phase transition behaviour [13,45].

The nature of both phase transitions,  $N_F$ - $N_S$  and  $N_S$ - $N$ , of RM734 is weakly first-order as discussed above. The  $N_S$ - $N$  anomaly is quite small and can only be detected in slow temperature scans. The larger and sharper  $N_F$ - $N_S$  phase transition exhibits several intriguing features. A tricritical (i.e.  $\alpha = 0.5$ ) effective exponent has been derived in a previous study [5]. We have also performed a few exploratory fits in reduced temperature ranges between  $10^{-4}$  and  $10^{-2}$ , yielding tricritical-like (i.e.  $\alpha \sim 0.5$ ) effective exponent values and critical amplitude ratios  $A_{NF}/A_{NS}$  between 0.22 and 0.34, depending on the range of fit. The obtained mean values of  $\alpha$  were very close when fitting both sides, whereas the errors were consistently larger at the  $N_F$  side, and were additionally correlated with the range of fit. At the critical point, the correlation length becomes very large and the system's behaviour universal. However, the  $N_F$ - $N_S$  transition is weakly first-order and its exact proximity to the tricritical point is unknown, thus, it could introduce these errors. Overall, our findings are in reasonable agreement with the results of Ref [5]; some minor differences could be related to the samples' origin and batch, as well as to the fitting of that work being done with a method that eliminates the influence of the background  $c_p$  [5,47]. However, both the current results and those reported in Ref. [5]. demonstrate the existence of larger pretransitional fluctuations above  $T_{NF-NS}$ . This marks an inverted Landau behaviour for the  $N_F$ - $N_S$  phase transition, as a classical Landau model predicts no pretransitional fluctuations at the high-temperature phase. Such behaviour is seldom present in LC phase transitions; it has previously been observed by AC calorimetry in transitions between different types of smectic-A [48] and smectic-C phases [49]. Interestingly, these smectic-A and smectic-C layered structures also exhibited periodical modulations of the dipole orientations. The similarity of the structure of these materials to RM734 should be noted; the reversed carboxylate ester orientation coupled with longer chain length yielded a rich smectic polymorphism.

A similar inverted Landau behaviour has also been encountered, being even more pronounced, in the  $N_F$ - $N_S$  phase transition of DIO [6]. The latter is also characterised by a different effective critical exponent  $\alpha = 0.88$  compared to RM734 ( $\alpha = 0.5$ ).

Some experimental data of the polarisation, birefringence, and dielectric permittivity of RM734 and DIO exist in the recent literature [9,12,14], albeit without any derivation of the relevant critical exponents. Therefore, the different values of  $\alpha$  reported so far, and the lack of information regarding the other critical exponents ( $\beta$  of the order parameter,  $\gamma$  of the susceptibility, and  $\nu$  of the correlation length) suggest that we are far from reaching a consensus about the critical behaviour of this transition in FNLCs.

## Conclusions

We have presented calorimetric and optical signatures of the intermediate, splay-nematic phase  $N_S$ , existing between the  $N$  and the  $N_F$  phases of RM734. Two samples from different batches have been used, originating from the University of Leeds, UK. The specific heat capacity profiles obtained by AC calorimetry have marked two transitions,  $N_F$ - $N_S$  and  $N_S$ - $N$ , upon heating and cooling. An average range of  $N_S$  phase of  $\Delta T_{NS} = 1.07 \pm 0.12$  K has been derived by AC calorimetry and  $\Delta T_{NS} = 1.2 \pm 0.3$  K by POM, in close agreement with previous measurements by Thoen et al. [8] on various samples of different origins. The  $N_S$  phase is detected in both bulk ( $\sim 1$  mm thick in AC calorimetry) and thin samples (a few  $\mu\text{m}$  thick in POM). The temperatures where the two transitions appear, show variations between samples of different origins and batches [8]. It is worth noting that the relative stability range of these phases is impacted by the amount of ionic impurities in the sample, as it has been recently proposed theoretically [50] and explored experimentally [13,45]. In particular, an increased  $N_S$  (or  $\text{SmZ}_A$ ) temperature stability range is reported when doping FNLCs, such as RM734 and DIO, with moderate amounts of ionic liquids [13,45].

Both transitions,  $N_F$ - $N_S$  and  $N_S$ - $N$ , of FNLCs, are weakly first-order as shown in the present work and other recent reports [6,8,51]. High-resolution calorimetry has revealed substantial critical fluctuations of the specific heat capacity above  $T_{NF-NS}$  for RM734 and DIO. Although such inverted Landau-like behaviour has been previously observed in phase transitions between smectic phases [48,49], it is – to the best of the authors' knowledge – observed for the first time in phase transitions between nematic phases. Regarding the  $N_F$ - $N_S$  anomaly, quite different effective critical exponent  $\alpha$  values have been reported: they are tricritical for RM734, whereas they do not belong to any known universality class for DIO. The values of other critical exponents have not yet been reported for any of the phase transitions occurring in FNLCs, and the characterisation of their critical behaviour calls for further experimental work.



## Acknowledgements

G.C. wishes to acknowledge stimulating discussions with J. Thoen and A. Erkořeka on ferroelectric nematics. M.L. and G. C. acknowledge financial support from Project P1-0125 of the Slovene Research and Innovation Agency. A.M. and N.S. acknowledge financial support of the Slovenian Research and Innovation Agency (P1-0192 and J1-50004). R.J.M. thanks UKRI for ongoing funding via a Future Leaders Fellowship, grant number MR/W006391/1.




## Disclosure statement

No potential conflict of interest was reported by the author(s).

## Funding

This work was supported by Slovenian Research and Innovation Agency.

## ORCID

Marta Lavrić  <http://orcid.org/0000-0003-3287-8910>  
 Nerea Sebastián  <http://orcid.org/0000-0002-9156-1895>  
 Calum J Gibb  <http://orcid.org/0000-0002-8626-4175>  
 Richard J Mandle  <http://orcid.org/0000-0001-9816-9661>  
 Alenka Mertelj  <http://orcid.org/0000-0002-2766-9121>  
 Nikola Novak  <http://orcid.org/0000-0002-1722-1702>  
 George Cordoyiannis  <http://orcid.org/0000-0001-5062-5322>

## References

- [1] Debye P. Some results on a kinetic theory of insulators. *Phys Z.* 1912;13:97–100.
- [2] Born M. About anisotropic liquids. Attempt of a theory of liquid crystals and the electric kerr effect in liquids. *Sitzungsber Preuss Akad Wiss.* 1916;30:614–650.
- [3] Mandle RJ, Cowling SJ, Goodby JW. A nematic to nematic transformation exhibited by a rod-like liquid crystal. *Phys Chem Chem Phys.* 2017;19(18):11429–11435. doi: 10.1039/C7CP00456G
- [4] Nishikawa H, Shirishita K, Higruchi H, et al. A fluid liquid-crystal material with highly polar order. *Adv Mater.* 2017;29(43):1702354. doi: 10.1002/adma.201702354
- [5] Thoen J, Korblova E, Walba DM, et al. Precision adiabatic scanning calorimetry of a nematic – ferroelectric nematic phase transition. *Liq Cryst.* 2022;49(6):780–789. doi: 10.1080/02678292.2021.2007550
- [6] Thoen J, Cordoyiannis G, Jiang W, et al. Phase transitions study of the liquid crystal DIO with a ferroelectric nematic, a nematic and an intermediate phase and of mixtures with the ferroelectric nematic compound RM734 by adiabatic scanning calorimetry. *Phys Rev E.* 2023;1107(1):014701. doi: 10.1103/PhysRevE.107.014701
- [7] Sebastián N, Čopič M, Mertelj A. Ferroelectric nematic liquid-crystalline phases. *Phys Rev E.* 2022;106(2):021001. doi: 10.1103/PhysRevE.106.021001
- [8] Thoen J, Cordoyiannis G, Korblova E, et al. Calorimetric evidence for the existence of an intermediate phase between the ferroelectric nematic phase and the nematic phase in the liquid crystal RM734. *Phys Rev E.* 2024;110(1):014703. doi: 10.1103/PhysRevE.110.014703
- [9] Chen X, Korblova E, Dong D, et al. First-principles experimental demonstration of ferroelectricity in a thermotropic nematic liquid crystal; polar domains and striking electro-optics. *Proc Natl Acad Sci USA.* 2020;117(25):14021–14031. doi: 10.1073/pnas.2002290117
- [10] Mertelj A, Cmok L, Sebastián N, et al. Splay nematic phase. *Phys Rev X.* 2018;8(4):041025. doi: 10.1103/PhysRevX.8.041025
- [11] Sebastián N, Cmok L, Mandle RJ, et al. Ferroelectric-ferroelastic phase transition in a nematic liquid crystal. *Phys Rev Lett.* 2020;124(3):037801. doi: 10.1103/PhysRevLett.124.037801
- [12] Chen X, Martinez V, Korblova E, et al. The smectic Z<sub>A</sub> phase: antiferroelectric smectic order as a prelude to the ferroelectric nematic. *Proc Natl Acad Sci USA.* 2023;120(8):e2217150120. doi: 10.1073/pnas.2217150120
- [13] Medle Pupnik P, Hanžel E, Lovšin M, et al. Antiferroelectric order in nematic liquids: flexoelectricity versus electrostatics. *Adv Sci.* 2025;24(9):2414818. doi: 10.1002/advs.202414818
- [14] Brown S, Cruickshank E, Storey JMD, et al. Multiple polar and non-polar nematic phases. *Chem Phys Chem.* 2021;22(24):2506–2510. doi: 10.1002/cphc.202100644
- [15] Manabe A, Bremer M, Kraska M. Ferroelectric nematic phase at and below room temperature. *Liq Cryst.* 2021;48(8):1079–1086. doi: 10.1080/02678292.2021.1921867
- [16] Cruickshank E, Walker R, Storey JMD, et al. The effect of a lateral alkyloxy chain on the ferroelectric nematic phase. *RSC Adv.* 2022;12(45):29482–29490. doi: 10.1039/D2RA05628C
- [17] Gibb CJ, Mandle RJ. New RM734-like fluid ferroelectrics enabled through a simplified protecting group free synthesis. *J Mater Chem C.* 2023;11(48):16982–16991. doi: 10.1039/D3TC03134A
- [18] Mandle RJ. A new order of liquids: polar order in nematic liquid crystals. *Soft Matter.* 2022;18(27):5014–5020. doi: 10.1039/D2SM00543C
- [19] Novotná V, Leicek L, Podoliak N. Twisted domains in ferroelectric nematic liquid crystals. *J Mol Liq.* 2024;403:124873. doi: 10.1016/j.molliq.2024.124873
- [20] Hobbs J, Gibb CJ, Mandle RJ. Emergent antiferroelectric ordering and the coupling of liquid crystalline and polar order. *Small Sci.* 2024;4:2400189. doi: 10.1002/smss.202400189
- [21] Cruickshank E. The emergence of a polar nematic phase: a Chemist's insight into the ferroelectric nematic phase. *Chem Plus Chem.* 2024;89(5):e202300726. doi: 10.1002/cplu.202300726
- [22] Gibb CJ, Hobbs J, Mandle RJ. Systematic fluorination is a powerful design strategy toward fluid molecular



- ferroelectrics. *J Am Chem Soc.* **2025**;147(5):4571–4577. doi: [10.1021/jacs.4c16555](https://doi.org/10.1021/jacs.4c16555)
- [23] Cruickshank E, Walker R, Strachan G, et al. The role of fluorine substituents on the formation of the ferroelectric nematic phase. *J Mater Chem C.* **2025**;13(8):3902–3916. doi: [10.1039/D4TC03318C](https://doi.org/10.1039/D4TC03318C)
- [24] Saha R, Nepal P, Feng C, et al. Multiple ferroelectric nematic phases of a highly polar liquid crystal compound. *Liq Cryst.* **2022**;49(13):1784–1796. doi: [10.1080/02678292.2022.2069297](https://doi.org/10.1080/02678292.2022.2069297)
- [25] Panarin JP, Jiang W, Yadav N, et al. Colossal dielectric permittivity and superparaelectricity in phenyl pyrimidine based liquid crystals. *J Mat Chem C.* **2025**;13(3):1507–1518. doi: [10.1039/D4TC03561E](https://doi.org/10.1039/D4TC03561E)
- [26] Rosseto MP, Selinger SV. Theory of the splay nematic phase: single versus double splay. *Phys Rev E.* **2020**;101(5):052707. doi: [10.1103/PhysRevE.101.052707](https://doi.org/10.1103/PhysRevE.101.052707)
- [27] Etxebarria J, Folcia CL, Ortega J. Generalization of the Mairt-Saupe theory to the ferroelectric nematic phase. *Liq Cryst.* **2022**;49(13):1719–1724. doi: [10.1080/02678292.2022.2055181](https://doi.org/10.1080/02678292.2022.2055181)
- [28] Szydłowska J, Majewski P, Čepič M, et al. Ferroelectric nematic-isotropic liquid critical end point. *Phys Rev Lett.* **2023**;130(21):216802. doi: [10.1103/PhysRevLett.130.216802](https://doi.org/10.1103/PhysRevLett.130.216802)
- [29] Erkoreka A, Martinez-Perdiguero J. Constraining the value of the dielectric constant of the ferroelectric nematic phase. *Phys Rev E.* **2024**;110(2):L022701. doi: [10.1103/PhysRevE.110.L022701](https://doi.org/10.1103/PhysRevE.110.L022701)
- [30] Matsukizono H, Sakamoto Y, Okumura Y, et al. Exploring the impact of linkage structure in ferroelectric nematic and smectic liquid crystals. *J Phys Chem Lett.* **2024**;15(15):4212–4217. doi: [10.1021/acs.jpcclett.3c03492](https://doi.org/10.1021/acs.jpcclett.3c03492)
- [31] Lavrentovich OD. Ferroelectric nematic liquid crystal, a century in waiting. *Proc Natl Acad Sci USA.* **2020**;117(26):14629–14631. doi: [10.1073/pnas.2008947117](https://doi.org/10.1073/pnas.2008947117)
- [32] Feng C, Saha R, Korblova E, et al. Electrically tunable reflection color of chiral ferroelectric nematic liquid crystals. *Adv Optical Mater.* **2021**;9(22):2101230. doi: [10.1002/adom.202101230](https://doi.org/10.1002/adom.202101230)
- [33] Caimi F, Nava G, Barboza R, et al. Surface alignment of ferroelectric nematic liquid crystals. *Soft Matter.* **2021**;17(35):8130–8139. doi: [10.1039/D1SM00734C](https://doi.org/10.1039/D1SM00734C)
- [34] Ortega J, Folcia CL, Etxebarria J, et al. Ferroelectric chiral nematic liquid crystals: new photonic materials with multiple bandgaps controllable by low electric fields. *Liq Cryst.* **2022**;49(15):2128–2136. doi: [10.1080/02678292.2022.2104949](https://doi.org/10.1080/02678292.2022.2104949)
- [35] Zavvou E, Klasen-Memmer M, Manabe A, et al. Polarisation-driven magneto-optical and nonlinear-optical behaviour of a room-temperature ferroelectric nematic phase. *Soft Matter.* **2022**;18(46):8804–8812. doi: [10.1039/D2SM01298G](https://doi.org/10.1039/D2SM01298G)
- [36] Caimi F, Nava G, Fuscetto S, et al. Fluid superscreening and polarization following in confined ferroelectric nematics. *Nat Phys.* **2023**;19(11):1658–1666. doi: [10.1038/s41567-023-02150-z](https://doi.org/10.1038/s41567-023-02150-z)
- [37] Sultanov V, Kavčič A, Kokkinakis E, et al. Tunable entangled photon-pair generation in a liquid crystal. *Nature.* **2024**;631(8020):294–299. doi: [10.1038/s41586-024-07543-5](https://doi.org/10.1038/s41586-024-07543-5)
- [38] Adaka A, Guragain P, Perera K, et al. Low field electrocaloric effect at isotropic–ferroelectric nematic phase transition. *Soft Matter.* **2025**;21(3):458–462. doi: [10.1039/D4SM00979G](https://doi.org/10.1039/D4SM00979G)
- [39] Basnet B, Paladugu S, Kurochkin O, et al. Periodic splay Fréedericksz transitions in a ferroelectric nematic. *Nat Commun.* **2025**;16(1):1444. doi: [10.1038/s41467-025-55827-9](https://doi.org/10.1038/s41467-025-55827-9)
- [40] Nishikawa H, Salamon P, Máthé MT, et al. Giant electro-viscous effects in polar fluids with paraelectric–modulated antiferroelectric–ferroelectric phase sequence. *arXiv.* **2025**. doi: [10.48550/arXiv.2502.05929](https://doi.org/10.48550/arXiv.2502.05929)
- [41] Yao H, Ema K, Garland CW. Nonadiabatic scanning calorimeter. *Rev Sci Instrum.* **1998**;69(1):172–178. doi: [10.1063/1.1148492](https://doi.org/10.1063/1.1148492)
- [42] Sigdel KP, Iannacchione GS. Calorimetric study of the nematic to smectic-A phase transition in octylcyanobiphenyl-hexane binary mixtures. *Phys Rev E.* **2010**;82(5):051702. doi: [10.1103/PhysRevE.82.051702](https://doi.org/10.1103/PhysRevE.82.051702)
- [43] Chan T, Garland CW, Nguyen HT. Calorimetric study of chiral liquid crystals with a twist-grain-boundary phase. *Phys Rev E.* **1995**;52(5):5000–5003. doi: [10.1103/PhysRevE.52.5000](https://doi.org/10.1103/PhysRevE.52.5000)
- [44] Cordoyiannis G, Lavrič M, Tzitzios V, et al. Experimental advances in Nanoparticle-Driven stabilization of liquid-crystalline blue phases and twist-grain boundary phases. *Nanomaterials.* **2021**;11(11):2968. doi: [10.3390/nano11112968](https://doi.org/10.3390/nano11112968)
- [45] Zhong B, Shuai M, Chen X, et al. Thermotropic reentrant isotropy and induced smectic antiferroelectricity in the ferroelectric nematic realm: comparing RM734 and DIO. *Soft Matter.* **2025**;21(6):1122–1133. doi: [10.1039/D4SM01008F](https://doi.org/10.1039/D4SM01008F)
- [46] Chen X, Zhu ZJ, Magrini M, et al. Ideal mixing of paraelectric and ferroelectric nematic phases in liquid crystals of distinct molecular species. *Liq Cryst.* **2022**;49(11):1531–1544. doi: [10.1080/02678292.2022.2058101](https://doi.org/10.1080/02678292.2022.2058101)
- [47] Thoen J, Marynissen H, Van Dael W. Temperature dependence of the enthalpy and the heat capacity of the liquid-crystal octylcyanobiphenyl (8CB). *Phys Rev A.* **1982**;26(5):2886–2905. doi: [10.1103/PhysRevA.26.2886](https://doi.org/10.1103/PhysRevA.26.2886)
- [48] Ema K, Garland CW, Sigaud G, et al. Heat capacity associated with nematic-smectic-A1-smectic-A-smectic-A (crenelated)-smectic-A2 phase sequence. *Phys Rev A.* **1989**;39(3):1369–1375. doi: [10.1103/PhysRevA.39.1369](https://doi.org/10.1103/PhysRevA.39.1369)
- [49] Ema K, Nounesis G, Garland CW, et al. Calorimetric study of smectic polymorphism in octyloxyphenyl-nitrobenzoyloxy benzoate + decyloxyphenyl-nitrobenzoyloxy benzoate mixtures. *Phys Rev A.* **1989**;39(5):2599–2608. doi: [10.1103/PhysRevA.39.2599](https://doi.org/10.1103/PhysRevA.39.2599)
- [50] Paik L, Selinger JV. Flexoelectricity versus electrostatics in polar nematic liquid crystals. **2024**. doi: [10.48550/arXiv.2408.10347](https://doi.org/10.48550/arXiv.2408.10347)
- [51] Cruickshank E, Rybak P, Majewska MM, et al. To Be or not to Be polar: the ferroelectric and antiferroelectric nematic phases. *ASC Omega.* **2023**;8(39):36562–36568. doi: [10.1021/acsomega.3c05884](https://doi.org/10.1021/acsomega.3c05884)